Desalination and Water Treatment
www.deswater.com

doi: 10.5004/dwt.2023.29141

281 (2023) 255–264
January

Chicken bone ash as a cost-effective and efficient adsorbent for phenol removal from aqueous solution

Mariam E. Fawzy[a], Hussein M. Ahmed[b,*], Hossam F. Nassar[c]

[a]*Water Pollution Research Department, National Research Centre, P.O. Box: 12622, Dokki, Giza, Egypt, Tel.: +20 01226645605; Fax: +20 233367319; email: mariamemadeldin@hotmail.com Orcid ID: 0000-0002-0552-5581*
[b]*Housing and Building Research Center (HBRC), Egypt, Sanitary and Environmental Engineering Institute (SEI), Tel.: +20 01065869112; email: Hussein_fee@yahoo.com*
[c]*Environmental Science and Industrial Development Department, Faculty of Postgraduate Studies for Advanced Sciences, Beni-Sueif University, 62511 Beni-Sueif, Egypt, email: hossamnassarnrc@gmail.com*

Received 30 May 2022; Accepted 21 November 2022

ABSTRACT

Phenol is a highly toxic compound and widely produced from various industrial wastes. Removal of phenol by chicken bone ash (CBA) from an aqueous solution was studied. CBA was prepared and characterized by scanning electron microscope (SEM) and X-ray diffraction (XRD). The SEM analysis shows that the CBA has a rough and large porous surface with interconnected irregular shape cavities. The XRD proved that hydroxyapatite was the main component of the ash. Batch and column adsorption procedures were performed to study the adsorption process. Adsorbent weight, solution pH, initial concentration and contact time revealed that the use of 0.8 g CBA for 180 min, 94.4% of phenol was removed at initial concentration of 250 mg·phenol/L. The highest removal rate of CBA was achieved at pH value of 8.0; it reached 91.6%. Eight analytical models were investigated to study the performance of fixed-bed columns for phenol removal by the adsorption process. The best values obtained were for Log–Gompertz with R^2 = 0.8748. Langmuir isotherm constant with a coefficient of determination (R^2) = 0.9842 fits successfully the adsorption process. The experimental data obey the pseudo-second-order with R^2 = 0.9624 and phenol removal is attributed to chemical precipitation reaction. Cost analysis revealed that for the production of 0.1 kg of CBA about 0.77 $ is required. In conclusion, for pollutant removal, the CBA proved to be cost effective, sustainable and renewable compared with activated carbon.

Keywords: Adsorption; Chicken bone activated carbon; Fixed-bed column; Industrial wastewater; Langmuir isotherm model; Analytical models; Phenol

1. Introduction

Wastewater is a new added environmental constituent and it is globally increasing due to the vast human activities with the rapid population increase [1]. The discharge of untreated effluents into water bodies is a huge environmental problem facing the world. Especially, if the effluents are contaminated by toxic or hazardous substances such as heavy metals [2], phenolic compounds, dyes, POPs. Contamination by such toxic compounds leads to the damage of drinking water resources and/or aquatic ecosystem [3,4]. They are toxic to aquatic life and their discharge leads to the decrease of oxygen content in water [5]. Phenol is a prime contaminant as designated by the US Environmental Protection Agency (EPA). It is present in wastewater as a common pollutant. The concentration limit of phenol that complies with EPA regulations in wastewater is less than 1,000 μg/L [5]. Therefore; it must be treated before being

* Corresponding author.

discharged into the environment. Phenolic compounds are highly toxic due to low biodegradability; exposure to phenolic compounds causes serious diseases for the brain, eyes, liver and skin. Several industrial manufacturing processes discharge phenolic compounds and their derivatives such as: petrochemicals, oil-refining [6], resin, wood, paper and pulp, pesticides, tannery, plastics [7], pharmaceuticals [8], disinfectants and cosmetics [9].

Numerous conventional technologies have been applied for the remediation of phenolic compounds from wastewater, such as: distillation, wet air oxidation, activated sludge process, extraction, precipitation. Other, advanced methods were applied including: photo-oxidation, ozonation, Fenton reaction, enzymatic treatment, electrochemical oxidation [5], ion exchange, membrane separation, and electrodialysis [10]. Nowadays, development of new eco-friendly, economical and effective approaches are applied for the decontamination of hardly biodegradable pollutants [1]. Adsorption is a good alternative especially if it is carried out by using natural materials such as clay, animal bones, agricultural products [11,12], sand, dust [10], and natural zeolite [13]. The adsorption method is the preferred method for treatment of many types of pollutants. In the adsorption process, the pollutants can be transferred from the solution to the adsorbent surface without toxic intermediate production [11]. Ash can be produced from biomass via pyrolysis; it is a carbon-rich material, stable and abundant in raw sources [12]. It has countless advantages due to the presence of many functional active groups, permeability, high adsorption capacity, tremendous surface area, and low cost. The adsorption process using ash generated via different sources depends on the preparation process [7]. Hasanah et al. [14] investigate that adsorption process occur due to the asymmetry of the surface area of the adsorbate that leads to the capture of adsorbent matter. This physical process was successfully applied for the removal of mercury, cadmium, and lead from laboratory pharmaceutical wastewater using chicken bone ash ignited at 800°C. They achieved removal rates of 74.45%, 63.64%, 66.67%, 90.41%, 98.96% and 95.09% for chemical oxygen demand, total dissolved solids, total suspended solids, Hg, Cd and Pb, respectively. Yu et al. [5] achieved a remarkable adsorption capacity of 568 mg/g for phenol at an initial concentration of 500 mg/L using carbon ash with large surface area of 745 m^2/g obtained from food waste after pyrolysis and activation at 950°C. Yusoff et al. [1] studied the removal of acetaminophen generated in pharmaceutical wastewater by adsorption using chemically chicken bone waste with a removal rate of 93% at a dose of 0.1 from chicken bone ash (CBA) with a start-up concentration of 1,000 mg/L at pH 2 and 25°C at a contact time of 120 min. Fawzy et al. [8] studied the removal of phenol in pharmaceutical wastewater through sorption and hydroxylation in activated sludge process and UV-free surface reactor. They achieved 100% removal of phenol at 6 h of aeration in ASP. Ghiaci et al. [15] use a dose of 0.005 g CBA for the removal of cadmium, lead, zinc, and nickel from aqueous solutions. The removal percentage reached 75.45%, 100%, 74.34% and 23.28%, respectively. In the same study, CBA was applied for Ni, Cd, Zn, and Pb ions removal from Zayanderood River. It was contaminated by oil refineries, chemicals, steel, power plants, and other industries. The removal of metal ions reached 100% at a pH ranged from 7–8 [15].

Chicken-animal bone (CAB) is a solid waste with no economic value, widely available at a negligible cost [14]. Carbonization of CAB at high temperature was carried out to form bone ash. Bone ash is a potential adsorbent characterized by an associated large void space network that can be used to remove contaminants from wastewater [1]. In this study animal bone from chicken was prepared, fully characterized, and utilized for the removal of phenol from aqueous media via adsorption process. The bone ash was used as an efficient adsorbent due to its surface morphology and the presence of calcium hydroxyapatite (CHA) and hydroxyapatite (HA) as major elemental components. Batch adsorption experiments were carried out to determine the optimum conditions for phenol removal by CBA. In addition, a fixed-bed column study was performed to study phenol adsorption behavior to scale-up the technology for wastewater treatment. Furthermore, experimental data were investigated by eight analytical models. The model's acceptability was assessed by examining the coefficient of determination (R^2) and the breakthrough curves for phenol adsorption by fixed-bed column. Moreover, to investigate the mechanisms that control the adsorption process; pseudo-first-order and pseudo-second-order kinetic models were carried out.

2. Material and method

2.1. Preparation and characterization of chicken bone ash

Waste bones were collected from butchers, local houses and restaurants. The bones were physically scraped from the flesh portions, washed several times with distilled water and then boiled for 4 h using distilled water to eliminate meat and lipids residues. The cleaning process was repeated many times. Then, the cleaned bones were dried at 105°C for 2 h. The dried bones were crushed with a mortar and sieved using a mesh analyzer at a size 60–90 μm; the pH of bone particles was neutral. A total of 50 g of dried chicken bones were converted to activated carbon by ignition in a muffle furnace at 550°C for 60 min. The resulted chicken bone ash product was allowed to cool at room temperature, then washed with distilled water and dried at 105°C. Scanning electron microscope (SEM) was performed using SEM Model Quanta 250 FEG (field emission attracted with accelerating gun) voltage 30KV FEI Company (The Netherlands) to study the surface morphology of CBA. X-ray diffraction (XRD) was conducted by model (X'Pert Pro PANalytical–Manufactured by PANalytical B.V. Co., Netherlands (ISO 9001/14001 KEMA – 0.75160) to study the structure of CBA.

2.2. Phenol preparation

Phenol crystal, C_6H_5OH, with molecular weight of 94.11%, 99.5% purchased from LOBA Chemie (India) was used to prepare a stock phenol solution by dissolving 1,000 mg/L in 1 L of distilled water at room temperature. Phenol solution pH was adjusted using 0.01 N HCL or NaOH and measured by a calibrated pH meter (Jenway 3510).

2.3. Phenol analysis

Phenol concentration was measured using UV spectrophotometer PG Instruments Ltd., (T70+) at a wavelength of 510 nm according to the standard methods [16,17]. Double-checking of phenol concentrations was performed for all samples.

2.4. Batch adsorption experiments

Phenol adsorption studies were performed in triplicates at ambient room temperature (25°C ± 2°C) by agitating 500 mL of the prepared synthetic phenol solutions at fixed dose of CBA with initial phenol concentrations of 250 mg/L and 30 min reaction time at pH 7 contained in 1,000 mL plastic Erlenmeyer flasks. The samples were analyzed to determine the phenol concentration after treatment. To study the adsorption behavior of phenol uptake by the chicken bone ash; solution pH 1.0, 3.0, 6.0, 8.0, and 10.0, effect of CBA dose 0.05, 0.1, 0.2, 0.5, 0.8, and 1.0 g, initial concentration of phenol 10, 100, 200, 400 and 500 mg/L and contact time 10, 30, 60, 90, 150, and 180 min at agitation rate 120 rpm were tested. The samples were removed from the shaker water bath (Lab Tech.), at appropriate intervals of time and then filtered with Whatman Filter Paper No. 41 and the remaining phenol concentration was determined. The amount of phenol adsorbed onto chicken bone ash was calculated according to Eqs. (1) and (2):

$$\text{The sorption percentage of phenol}\left(R\%\right)=\frac{C_o-C_t}{C_o}\times 100 \quad (1)$$

$$q_e\left(\text{mg/g}\right)=\frac{\left(C_o-C_t\right)V}{m} \quad (2)$$

where q_e (mg/g) is the number of pollutants adsorbed per unit weight of bone at equilibrium, C_o and C_t are the initial and final concentrations of phenol in aqueous solution, while V and m represent the volume of phenol solution (L) and weight of adsorbent (g).

2.5. Fixed-bed column experiment

Continuous adsorption experiments were performed using fixed-bed glass column, 50 cm in height and 5 cm in diameter, filled with 108.25 g CBA, packed into the glass column to make a suspension. The column was supported by cotton at the bottom to prevent the leakage of CBA from the column and the bed height was measured at the beginning (45 cm). Distilled water was passed through the adsorbent bed to remove impurities and air trapped in the adsorbents. A phenol concentration of 250 mg/L was passed in a down flow mode through the column with a flow rate of 5.0 mL/min to study the adsorption behavior. Effluents were collected at regular time intervals 10, 30, 60, 90, 120, 150 and 180 min and the breakthrough curves are plotted in terms of C_t/C_o vs. time.

2.6. Column isotherm

For evaluating the dynamic response of a fixed-bed adsorption process, the breakthrough time and curve shape were determined. By graphing R% phenol concentration vs. time, the breakthrough curve is used to describe phenol adsorption, concentration from the synthetic solution of phenol in the fixed-bed column, and is commonly given in terms of normalized output concentration. The stoichiometric time is used to determine the capacity at full equilibrium; as a result, the area above the breakthrough curve is equal to the area below the breakthrough curve. It can be calculated by Eq. (3).

$$q_e\left(\text{mg/g}\right)=\frac{C_o\times Q}{m}\int_0^t\left(C_o-C_{\text{ads}}\right)dt \quad (3)$$

The quantity of pollutants adsorbed per unit weight of bone at equilibrium is q_e (mg/g), the initial phenol concentration is C_o (mg/L), the adsorbed phenol concentration is C_{ads} (mg/L), the volumetric flow rate is Q (mL/min), t is time (min) and the adsorbent mass is m (g).

2.7. Modelling of fixed-bed adsorption column

Eight analytical models were used to study the behavior of phenol adsorption through a fixed-bed column and for scaling up for field applications. Bohart–Adams, Wolborska, Thomas, Yoon–Nelson, Log–Gompertz, Gompertz, Dose–Response, and bed depth service time (BDST) models were studied as follows [19].

2.7.1. Bohart–Adams model

The non-linear form of Bohart–Adams models is shown in Eq. (4). In fixed-bed column, it is employed to determine the initial condition of the surface operation. The model is based on the surface reaction theory. The adsorption rate is considered to be proportional to both the residual adsorbent capacity and the initial concentration of the adsorbent.

$$\frac{C_{\text{ads}}}{C_o}=\frac{1}{1+e^{\left(\alpha-B+t\right)}} \quad (4)$$

where $\alpha = k_{\text{BA}} \times N_o \times Z$ and $\beta = k_{\text{BA}} \times C_o \times t$. k_{BA} signifies the Bohart–Adams kinetic constant (L/mg·min). N_o and Z is the saturation concentration (mg/L) as well as the bed depth of the column (cm), respectively [20].

2.7.2. Yoon–Nelson model

It is used to describe the period of time during which the column runs before its replacement or recognition becomes mandatory. The Yoon–Nelson model assumes that the probability of adsorption of each molecule is directly proportional to the probability of adsorbate breakthrough on the adsorbent and the probability of adsorbate adsorption. The non-linear form of the model is given in Eq. (5) [18].

$$\frac{C_{\text{ads}}}{C_o}=\frac{e^{\left(KYN\times t-\tau\times KYN\right)}}{1+e^{\left(KYN\times t-\tau\times KYN\right)}} \quad (5)$$

where K is the kinetic constant (L/mg·min), N and Y is the saturation concentration in (mg/L) as well as the bed depth of the column (cm), respectively.

2.7.3. Thomas model

Thomas model is widely used to describe the column performance and to predict the breakthrough curves. The non-linear form of the model is represented in Eq. (6) [18].

$$\frac{C_{\text{ads}}}{C_o} = \left(\frac{K_{\text{th}} \times q_{\text{th}} \times m}{Q} - K_{\text{th}} \times C_o \times t \right) \tag{6}$$

where K_{th} represents the Thomas constant in (mL/min·mg), q_{th} denotes the uptake capacity calculated by Thomas model in (mg/g), m denotes the adsorbent mass in the column in (g), and Q represents the volume flow rate in (mL/min).

2.7.4. Wolborska model

Wolborska model describe the concentration distribution of the breakthrough curves at low concentrations of effluent. The non-linear form can be estimated from Eq. (7).

$$\frac{C_{\text{ads}}}{C_o} = e^{\left(\frac{\beta \times C_o}{N_o}\right) \times t - \left(\frac{B \times Z}{u}\right)} \tag{7}$$

where β is the external mass transfer coefficient (L/min), Z denotes the bed height in (cm); u is the superficial velocity in terms of flow rate over the cross-sectional area. N_o is the saturation concentration (mg/L) [18].

2.7.5. Gompertz model

Gompertz model is used to correlate asymmetric breakthrough data as a function of time as shown in Eq. (8).

$$\frac{C_{\text{ads}}}{C_o} = e^{-e^{-(\alpha - B \times t)}} \tag{8}$$

where α and β (L/min) represent the Gompertz model parameters [16,17].

2.7.6. Log–Gompertz model

Log–Gompertz model is a modified version of the Gompertz model, it provides breakthrough curves that resemble cumulative probability distributions, with the independent variable t set to log(t), enhancing the fit with breakthrough data. The Log–Gompertz model equation can be presented through Eq. (9) [18].

$$\frac{C_{\text{ads}}}{C_o} = e^{-e^{-(\alpha - B \times \log t)}} \tag{9}$$

2.7.7. Dose–Response model

Dose–Response model was used to explain the biosorption process as presented by Eq. (10) [18].

$$\frac{C_{\text{ads}}}{C_o} = 1 - \frac{1}{1 + \left(\frac{Q \times C_o \times t}{q_f \times m} \right) a} \tag{10}$$

where a is a constant and q_f represents the adsorption capacity provided by the modified Dose–Response model in (mg/g), C_o (mg/L) is the initial adsorbate concentration, Q (mL/min) denotes the volume flow rate, t is time and m (g) represents the adsorbent mass in the column.

2.7.8. BDST model

Bohart–Adams model is used for modelling of adsorption behavior in a fixed-bed column. It is a basic model that shows the relationship between process concentration, biosorption parameters, depth and time. The model is based on physical measurements of bed capacity at different breakthrough values. The BDST model is used to determine the required bed depth for a given service time (Eq. 11) [18].

$$\frac{C_{\text{ads}}}{C_o} = \frac{1}{1 + e^{\left(k_{\text{BDST}} \times C_o\right)\left(N_o / C_o \times Z - t\right)}} \tag{11}$$

where N_o denotes the adsorption capacity (mg/L) of a fixed-bed column, Z represents the bed height (cm) and k_{BDST} shows the adsorption rate constant that indicate the mass transfer from liquid to the solid phase (L/mg·min).

2.8. Kinetic study

In this study pseudo-first-order and pseudo-second-order kinetic models were used to investigate the mechanism that controls the overall removal rate in the adsorption process.

Pseudo-first-order is commonly used during the first 10–180 min of the sorption phase as shown in Eq. (12) [19,20].

$$\log\left(q_e - q_t\right) = \log q_e - \frac{k}{2.303} t \tag{12}$$

While pseudo-second-order kinetics assumes that the sorption process involves a chemisorption mechanism and the rate of site occupation is proportional to the square of the number of unoccupied sites as expressed in Eq. (13):

$$\frac{t}{q_t} = \frac{1}{kq^2} + \left(-\frac{t}{q_e} \right) \tag{13}$$

2.9. Adsorption isotherm

Langmuir and Freundlich isotherm models were used to describe the process equilibrium. The experimental data were correlated using the traditional Freundlich and Langmuir models. The Langmuir model assumes monolayer adsorption, whereas the Freundlich model implies heterogeneous adsorption on the surface [21]. Eqs. (14) and (15) respectively provide the linear form of Freundlich and Langmuir models:

Langmuir isotherm:

$$\frac{1}{q_e} = \frac{1}{q_{\max} K_L} \frac{1}{C_e} + \frac{1}{q_{\max}} \tag{14}$$

Freundlich isotherm

$$\log q_e = \log K_f + \frac{1}{n} \log C_e \tag{15}$$

where q_e (mg/g) is the amount of pollutants adsorbed per unit weight of bone at equilibrium, C_e is the residual concentration of pollutants in the solution at equilibrium (mg/L), $q_{\max}$ is the amount of pollutants adsorbed per unit of adsorbent for a monolayer surface (mg/g), K and n are Freundlich constants that were obtained from the slope and intercept of the plots of each isotherm, K is the Langmuir constant (L/mg).

3. Results and discussion

3.1. Characterization of chicken bone activated carbon

3.1.1. Surface morphology of CBA

SEM was performed to recognize the surface morphology of the CBA. Fig. 1a and b illustrate the SEM morphology for samples at low and high magnification, respectively. All samples displayed cavity frameworks with interconnecting irregular shaped cavities, which resulted from the elimination of unstable composites during carbonization [22]. The CBA surface is heterogeneous [20]. The presence of pores in surface of CBA aids in the adsorption of large molecules with a high adsorption uptake [21,23]. SEM analysis shows that the CBA had a rough and porous surface. Thus, there is evidence that CBA can be used as an adsorbent for phenol removal in aqueous media [24,25].

3.1.2. XRD elemental analysis of CBA

XRD was performed to assess the crystallographic structural properties and phase purity of the CBA obtained from chicken bones. Figs. 2 and 3 illustrate the XRD analysis of chicken bone waste and CBA, while the chemical composition is shown in Table 1. Results of XRD analysis showed that raw bone is mainly composed of calcium carbonate ($CaCO_3$) as calcite. While, for CBA the main components were calcium and phosphorus as hydroxyapatite ($Ca_{10}(OH)_2(PO_4)_6$) [24,25]. The XRD analysis indicated the crystalline structure of chicken bone. Calcium carbonate (calcite) was identified in the spectrum of CBA and this may be attributed to the decay of non-stoichiometric carbonate after combustion containing apatite bone and assigned to hydroxyapatite. In addition, a peak from $Ca_{10}(PO_4)_6(OH)_2$ appeared [26,27] due to the presence of PO_4^{3-} and OH^- peaks [28]. Furthermore, the diffraction patterns of the crystalline

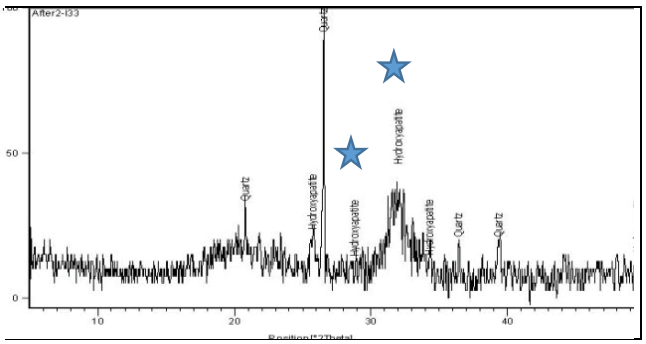

Fig. 2. XRD for chicken bone waste.

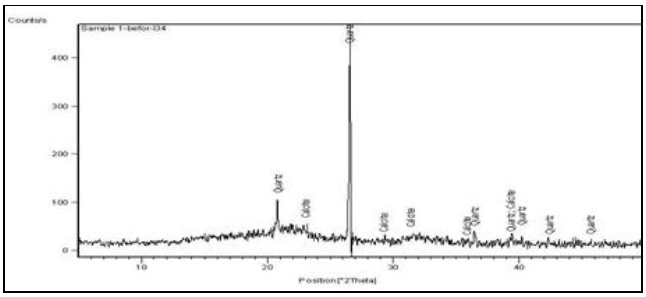

Fig. 3. XRD for chicken bone ash.

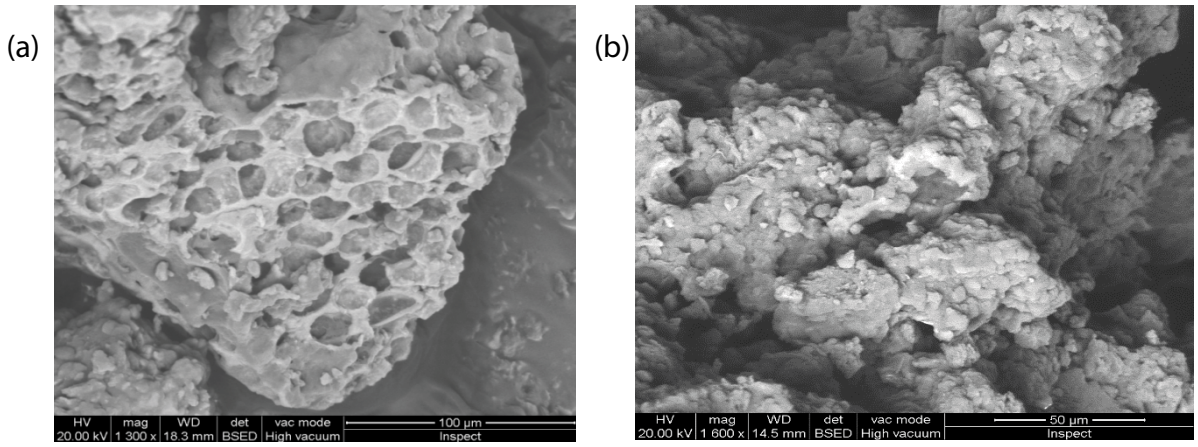

Fig. 1. SEM of CBA (a) before and (b) after treatment.

form of hydroxyapatite were observed in the XRD results of the CBA. Reflections in the figure can be indexed to 002 and 10 of graphite (JCPDS Card Files, No. 41-1487). The (002) peak at 26.1° is shifted slightly from 2θ = 26.4° for graphite, corresponding to an increase in the spacing between the sp2 carbon layers from 0.337 nm for graphite to 0.341 nm for CNPs [29]. Also, the broad 10 diffraction originates from a two-dimensional lattice. In summary, the bio-adsorbent diffraction pattern is similar to that recorded for other bone ash obtained from bovine, porcine, and animal bones [30].

3.2. Effect of pH, contact time, CBA dose and initial phenol concentration

Batch mode operation was used to study the adsorption of phenol elimination by CBA. The effect of pH is depicted in Fig. 4, the maximum uptake of phenol increased from 3.6% at acidic pH up to 91.6% at pH 8 and this was achieved after 90 min contact time and CBA dose of 0.8 g at 120 rpm. This can be attributed to the electrostatic interaction between phenol molecules and the negatively charged surface area of CBA which facilitates the adsorption capacity [13]. Increasing pH to 9 decreases the capacity of phenol adsorption by CBA to 73.6%. To study the effect of time on phenol adsorption, different contact time starting from 10 min up to 180 min was studied. The findings showed that as the contact time increases, the adsorption capacity of phenol increases, as shown in Fig. 5. The maximum phenol removal was obtained at 180 min with a removal rate of 95.2%. Phenol adsorption rate after 30 min was rapid and this was in agreement with [31]. Rapid adsorption of phenol was achieved due to the external adsorption on the surface of CBA where many active sites exist and are available for phenol adsorption [26]. The equilibrium was achieved after 150 min and the same behavior was noticed by Al-Tohami et al. [29]. At equilibrium, internal adsorption is approached inside CBA. Fig. 6 shows the effect of CBA dose on phenol removal. The dose of CBA ranged from 0.05 to 1 g with an initial phenol concentration (10–500 mg/L); increasing the CBA dose increases the removal rate of phenol. At a dose of 0.8 g, the removal of phenol reached 94.4%. It is clear from the results that the adsorption process is directly proportional to the dose of chicken bone ash. At an initial concentration of 400 mg·phenol/L, a high adsorption capacity of 188.12 mg/g was achieved. This might be attributed to increasing the dose of CBA (mass adsorbent) leading to more active sites for the uptake of phenol on the CBA surface [30]. The effect of initial phenol concentration is depicted in Fig. 7. It was obvious that raising the concentration of phenol up to 500 mg/L decreased the removal rate to 51.4%. This may be attributed to higher concentrations of phenol, the driving force increase between the CBA pores and phenol leading to the prevention of phenol, passing inside the mass adsorbent [5] and the saturation of CBA vacant sites at high phenol concentration occurs.

Table 1
Chemical composition of raw bone, and chicken bone activated carbon (CBA)

Item	XRD of raw bone	XRD of CBA at 550°C
Calcite ($CaCO_3$), Max. count/s	20	0
Hydroxyapatite ($Ca_{10}(OH)_2(PO_4)_6$), Max. count/s	0	40

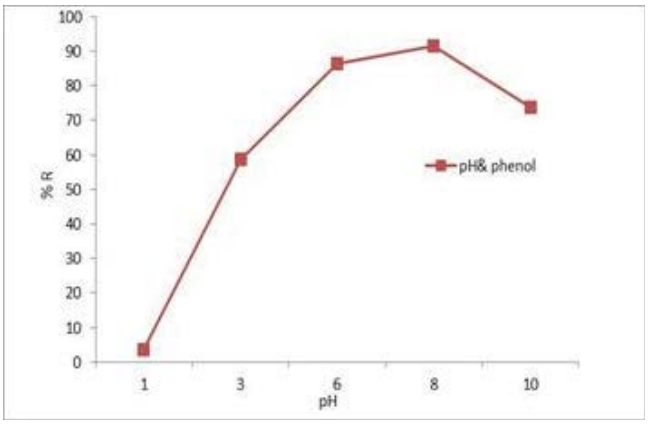

Fig. 4. Effect of pH on phenol removal.

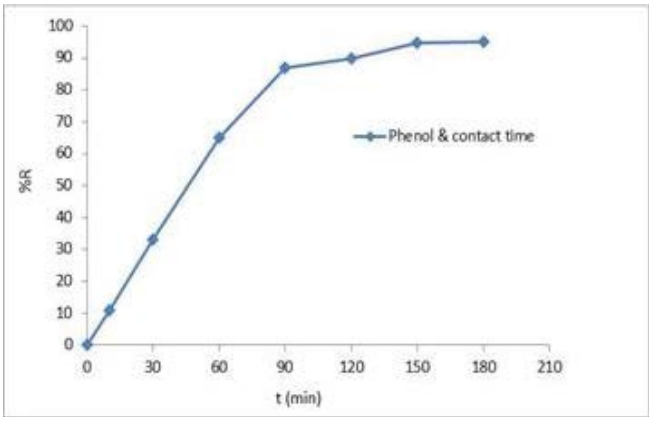

Fig. 5. Effect of contact time on phenol removal.

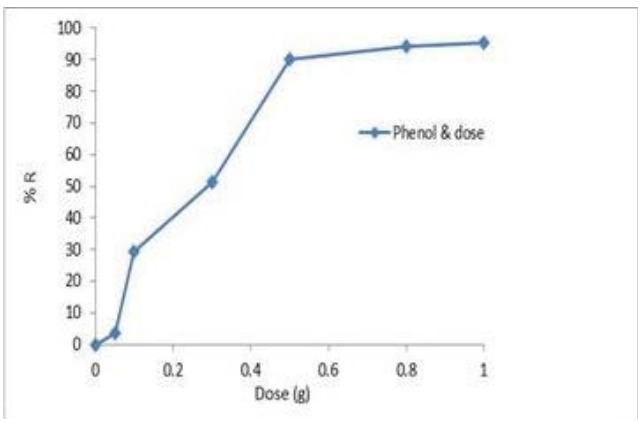

Fig. 6. Effect of CBA dose on phenol removal.

3.3. Mathematical modeling of breakthrough curves

Fixed-bed column process is performed to study the removal of inorganic and organic matter from wastewater. To study the performance of fixed-bed column for phenol removal by adsorption process, eight analytical models were validated. Breakthrough curves were calculated for bed depth service time, Gompertz, Wolborska, Bohart–Adams, Thomas, Yoon–Nelson, Gompertz and Dose–Response as shown in Figs. 8–11. The data obtained revealed that the experimental results fit and respond well to each model by calculating the coefficient of determination. The behavior of BDST, Bohart–Adams and Dose–Response was exactly analogous with a R^2 value of 0.8171. While, for Thomas, Yoon–Nelson, Wolborska and Gompertz was 0.8565. However, the best values observed were for Log–Gompertz with R^2 = 0.8748 as shown in Fig. 11 with sigmoidal shape. Log–Gompertz equation is a simple mathematical model used for the determination of the maximum growth rate such as substrate consumption, growth process, and biogas production in anaerobic digestion for wastewater treatment [32]. Also, no clear relation between the volume and bed height (h) was detected but related to the initial concentration and the flow rate. This phenomenon is expected since more concentration implies more solute per time unit traveling in the column. Thus, the full mechanism of phenol adsorption can't be clearly estimated by mathematical models, and this is in agreement with Anisuzzaman et al. [33] but they are used to determine the design parameters for column studies and to scale-up the application of phenol adsorption by CBA.

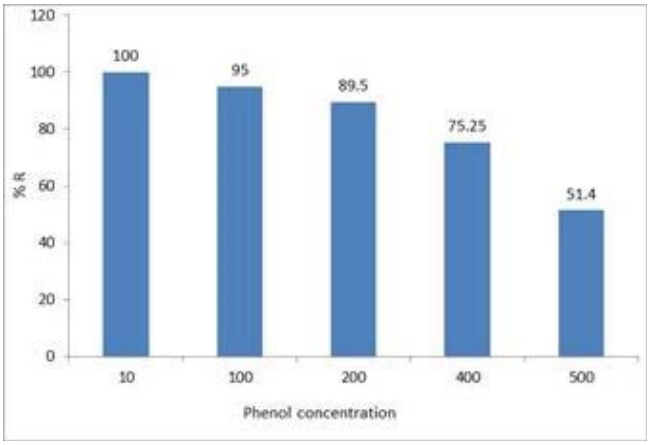

Fig. 7. Effect of initial phenol concentration.

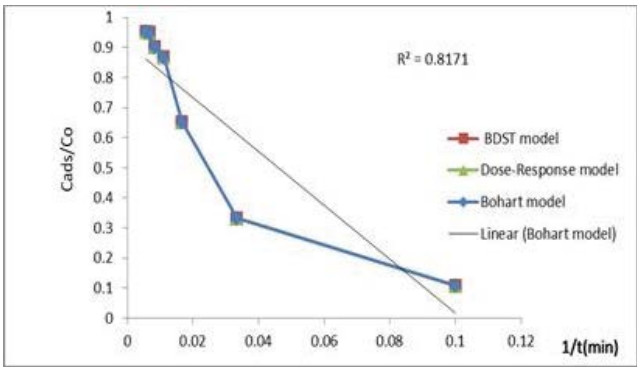

Fig. 8. Bohart–Adams, Dose–Response and BDST models breakthrough curves for phenol adsorption.

3.4. Adsorption kinetics

Kinetic models were applied to predict the time needed to reach the equilibrium phase and to determine the maximum adsorption capacity. A coefficient of determination (R^2) was calculated for each model via non-linear regression.

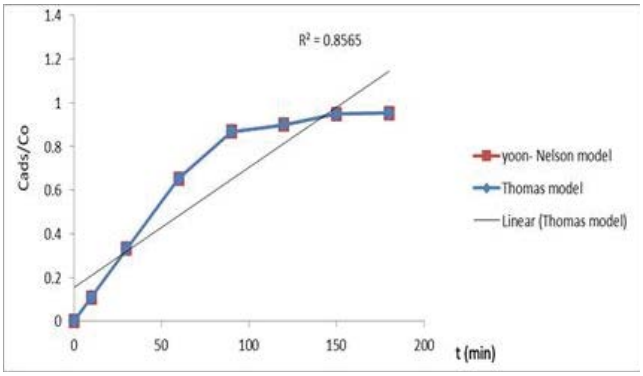

Fig. 9. Yoon–Nelson and Thomas models breakthrough curves for phenol adsorption.

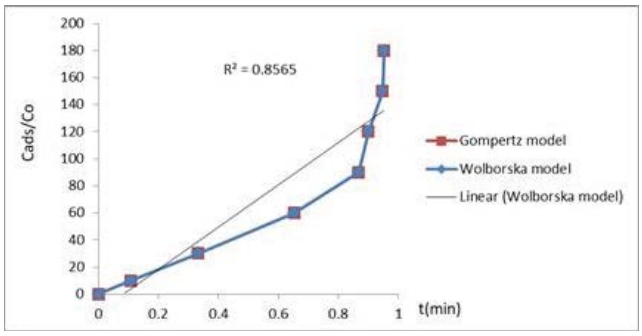

Fig. 10. Wolborska and Gompertz models breakthrough curves for phenol adsorption.

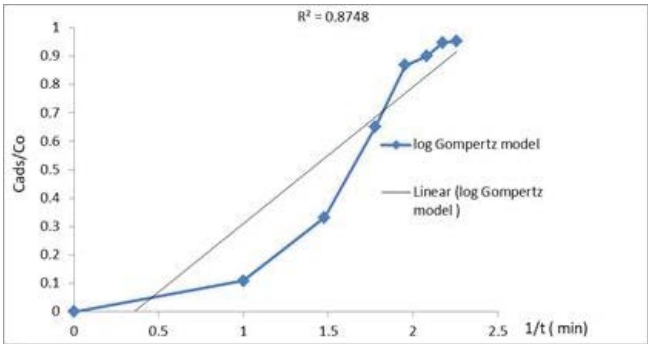

Fig. 11. Log–Gompertz model breakthrough curves for phenol adsorption.

The results illustrated in Figs. 11 and 12 showed that phenol adsorption follows the pseudo-second-order kinetics with R^2 of 0.9624. The mechanism of phenol removal is attributed to a chemical precipitation reaction. CBA analysis proved that the inorganic structure of chicken bone consists mainly of $Ca_{10}(PO_4)_6(OH)_2$ (HAP: hydroxyapatite). Where, the inter-changeable and the hydroxides were replaced by phenol, forming an insoluble precipitate indicating the formation of phenol-apatite (PAP) as a precipitate compound [24] as shown in Eq. (16).

$$Ca_{10}(PO_4)_6(OH)_2 + OH\text{--}C_6H_5 \rightarrow Ca_{10}(PO_4)_6(OH)\text{---}O\text{---}C_6H_5 + H_2O \quad (16)$$

3.5. Adsorption isotherm

Langmuir and Freundlich isotherm constants were investigated by non-linear regression. The data presented in Figs. 14 and 15 revealed that Langmuir model fits successfully the adsorption of phenol on CBA. Reaching equilibrium phase, as the initial phenol concentration increase, the adsorption capacity increases. At an initial concentration of 400 mg·phenol/L; the maximum adsorption capacity was 188.12 mg/g. A coefficient of determination was calculated with a value of 0.9842 and this proves that phenol removal did not obey the pore-filling mechanism. Phenol adsorption was performed by monolayer adsorption mechanism on the surface of CBA where the available active sites were unlikely [34].

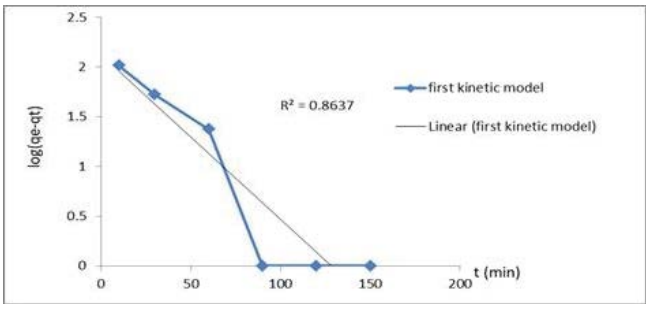

Fig. 12. Pseudo-first-order kinetic of phenol adsorption on CBA.

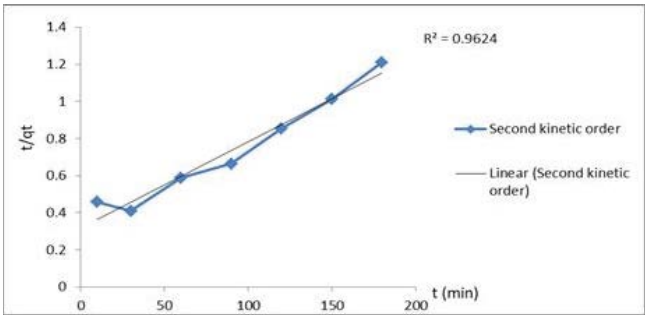

Fig. 13. Pseudo-second-order kinetic of phenol adsorption on CBA.

3.6. Materials, energy consumption and cost analysis

Based on the preparation process used in this study, the cost analysis of using chicken bone ash as an effective adsorbent of phenol from aqueous solution was calculated as shown in Table 2. The cost analysis shows that the specific energy consumption of the adsorbent production is 14.79 kWh/m^3 and for water consumption is 0.0065 m^3. The cost required for the production of 0.1 kg of CBA is

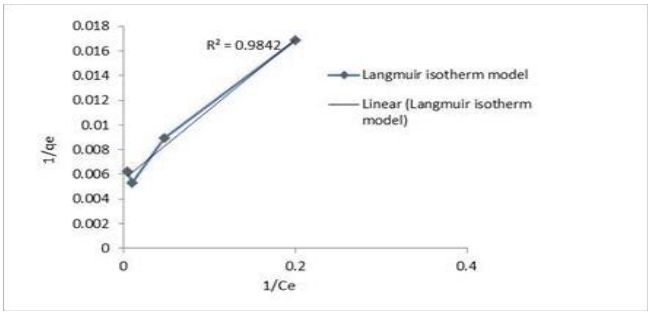

Fig. 14. Isotherm of phenol adsorption by CBA with Langmuir model.

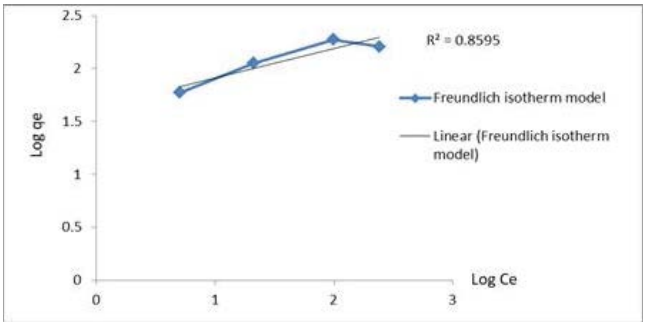

Fig. 15. Isotherm of phenol adsorption by CBA with Freundlich model.

Table 2
Material and energy consumption for production 0.1 kg of ash material

Process	Water consumption (m^3)[a]	Electricity consumption (kWh)[b]
Washing	0.002	–
Washing with hot water	0.001	2
Drying at 105°C (2 h)	–	2
Crushing	–	0.5
Washing	0.0015	–
Burning at 550°C (1 h)	–	3.7
Washing	0.002	–
Drying at 105°C (2 h)	–	2
Total consumption	0.0065	10.2
Cost	0.065	14.79

[a]In Egypt, the cost of 1 m^3 of water for industrial use = 10.0 LE;
[b]In Egypt, the cost of 1 kWh of electricity for industrial use = 1.45 LE.

14.855 Egyptian Pound, which is equivalent to 0.77 $ (current exchange rate). This is considered to be very low value since CBA is produced from waste material at a priceless cost compared with other adsorbents such as activated carbon or any other adsorbents [32]. Besides being cost-effective, the treatment method for hazardous pollutants such as phenol and the adsorption process is environmentally friendly and does not generate a secondary by-product. The cost was calculated according to the following:

The cost for 0.1 kg of ash = cost of materials + cost of electricity consumed.

Hence, the cost = 0.065 + 14.79 = 14.855 LE (Egyptian pound) for the production of 0.1 kg.

3.7. Comparison of phenol removal with other studies

Table 3 shows some of the different methodologies carried out for phenol removal from the literature.

4. Conclusion

In this study, chicken bone ash (CBA) was collected from chicken bone waste, characterized and tested for phenol removal from aqueous media. The CBA was obtained by ignition at 500°C. SEM and XRD analysis showed that the CBA consist of hydroxyapatite with crystalline, porous structure. The effects of initial concentration of phenol, pH, dose of CBA and contact time on adsorption process were depicted. Kinetic study, isotherm and analytical models were evaluated. The results obtained emphasis that the adsorption process is directly proportional with the dose of CBA. Increasing the dose of CBA leads to more active available sites for the uptake of phenol on the surface. Also, the adsorption of phenol on CBA obeys the pseudo-second-order and Langmuir isotherm fits successfully with R^2 exceeds 0.95. The findings of this study, confirmed that chicken bone waste can be utilized as a food waste management practice to produce CB ash. It is a sustainable, renewable and priceless solution for the removal of hazardous substances from wastewater at even low concentrations compared to activated carbon.

Acknowledgements

This research did not receive any specific grant from funding agencies in the public, commercial, or not-for-profit sectors.

References

[1] N.A. Yusoff, N. Ngadi, H. Alias, M. Jusoh, Chemically treated chicken bone waste as an efficient adsorbent for removal of acetaminophen, Chem. Eng. Trans., 56 (2017) 925–930.
[2] S.I. Abou-Elela, S.A. El-Shafai, M.E. Fawzy, M.S. Hellal, O. Kamal, Management of shock loads wastewater produced from water heaters industry, Int. J. Environ. Sci. Technol., 15 (2017) 743–754.
[3] H.M. Ahmed, E.F. Mariam, F.N. Hossam, Effective chemical coagulation treatment process for cationic and anionic dyes degradation, Egypt. J. Chem., 65 (2022) 299–307.
[4] S.I. Abou-Elela, M.E. Fawzy, S.A. El-Shafai, Treatment of hazardous wastewater generated from metal finishing and electro-coating industry via self-coagulation: case study, Water Environ. Res., 93 (2021) 1476–1486.
[5] L. Yu, D.P. Gamliel, B. Markunas, J.A. Valla, A promising solution for food waste: preparing activated carbons for phenol removal from water streams, ACS Omega, 6 (2021) 8870–8883.
[6] H.F. Nassar, M.E. Fawzy, Evaluation of sand filter as a non-conventional post treatment of oil refinery wastewater: effect of flow rate, Egypt. J. Chem., 64 (2021) 3935–3942.
[7] M.C Lakshmi, V. Sridevi, A review on biodegradation of phenol from industrial effluents, J. Ind. Pollut. Control, 25 (2009) 13–27.
[8] M.E. Fawzy, I. Abdelfattah, M.E. Abuarab, E. Mostafa, K.M. Aboelghait, M.H. El-Awady, Sustainable approach for pharmaceutical wastewater treatment and reuse: case study, Environ. Sci. Technol., 11 (2018) 209–219.
[9] K.K. Thasneema, T. Dipin, M.S. Thayyil, P.K. Sahu, M. Messali, T. Rosalin, T.B. Hadda, Removal of toxic heavy metals, phenolic compounds and textile dyes from industrial waste water using phosphonium based ionic liquids, J. Mol. Liq., 323 (2021) 114645, doi: 10.1016/j.molliq.2020.114645.
[10] Z.Z. Ismail, H.N. AbdelKareem, Sustainable approach for recycling waste lamb and chicken bones for fluoride removal

Table 3
Comparison of phenol removal with other studies

Methodology	Results	References
Adsorption by granular activated carbon	93.4% removal was achieved, and the maximum adsorption capacity (q_{max}, mg/g) of 112.36	Leili et al. [35]
Adsorption by modified bentonite	92.22% removal was achieved, and the maximum adsorption capacity (q_{max}, mg/g) of 22.8	Leili et al. [35]
Biological treatment	100% removal was achieved by activated sludge process	Fawzy et al. [8]
Solar photocatalytic	99.4% removal was enhanced by ferrioxalate complex	Abid et al. [36]
Adsorption by modified clay	93.76% removal was achieved, and the maximum adsorption capacity (q_{max}, mg/g) of 18.8	Gładysz-Płaska [37]
Adsorption by agro-waste nanoparticles	>96% of phenol was achieved	Malakootian et al. [38]
CBA	94.4% removal was achieved, and the maximum adsorption capacity (q_{max}, mg/g) reached 188.12 at initial phenol concentration 400 mg/L, dose 0.8 g, 150 min, and 120 rpm	Present study

from water followed by reusing fluoride-bearing waste in concrete, Waste Manage., 45 (2015) 66–75.
[11] C. Arora, D. Sahu, D. Bharti, V. Tamrakar, S. Soni, S. Sharma, Adsorption of hazardous dye crystal violet from industrial waste using low-cost adsorbent *Chenopodium album*, Desal. Water Treat., 167 (2019) 324–332.
[12] C. Arora, P. Kumar, S. Soni, J. Mittal, A. Mittal, B. Singh, Efficient removal of malachite green dye from aqueous solution using *Curcuma caesia* based activated carbon, Desal. Water Treat., 195 (2020) 341–352.
[13] S.S. Alquzweeni, R.S Alkizwini, Removal of cadmium from contaminated water using coated chicken bones with double-layer hydroxide (Mg/Fe-LDH), Water, 12 (2020) 2303–2316.
[14] U. Hasanah, A. Iryani, A. Taufiq, D.A.D. Putra, Chicken bone based adsorbent for adsorption of Pb(II), Cd(II), and Hg(II) metals ion liquid waste, Helium: J. Appl. Chem., 1 (2021) 11–18.
[15] M. Ghiaci, N. Dorostkar, A. Gil, Chicken bone ash as an efficient metal biosorbent for cadmium, lead, nickel, and zinc from aqueous solutions, Desal. Water Treat., 52 (2014) 3115–3121.
[16] S. Mukherjee, S. Kumar, A.K. Misra, M. Fan, Removal of phenols from water environment by activated carbon, bagasse ash and wood charcoal, Chem. Eng. J., 129 (2007) 133–142.
[17] APHA, Standard Methods for the Examination of Water and Wastewater (23rd ed.), American Public Health Association, Washington D.C., 2017.
[18] H. Patel, Batch and continuous fixed-bed adsorption of heavy metals removal using activated charcoal from neem (*Azadirachta indica*) leaf powder, Sci. Rep., 10 (2020) 1–12.
[19] D. Juela, M. Vera, C. Cruzat, X. Alvarez, E. Vanegas, Mathematical modeling and numerical simulation of sulfamethoxazole adsorption onto sugarcane bagasse in a fixed-bed column, Chemosphere, 280 (2021) 130687, doi: 10.1016/j.chemosphere.2021.130687.
[20] M.C. Ncibi, B. Mahjoub, M. Seffen, Kinetic and equilibrium studies of methylene blue biosorption by *Posidonia oceanica* (L.) fibres, J. Hazard. Mater., 139 (2007) 280–285.
[21] H.I. Abdel-Shafy, M.M. Hefny, H.M. Ahmed, F.M. Abdel-Haleem, Removal of cadmium, nickel, and zinc from aqueous solutions by activated carbon prepared from corncob - waste agricultural materials, Egypt. J. Chem., 55 (2022) 677–687.
[22] D.J. Tarimo, K.O. Oyedotun, N.F. Sylla, A.A. Mirghni, N.M. Ndiaye, N. Manyala, Waste chicken bone-derived porous carbon materials as high performance electrode for supercapacitor applications, J. Energy Storage, 51 (2022) 104378, doi: 10.1016/j.est.2022.104378.
[23] A.A. Ahmad, B.H. Hameed, A.L. Ahmad, Removal of disperse dye from aqueous solution using waste-derived activated carbon: optimization study, J. Hazard. Mater., 170 (2009) 612–619.
[24] E. Haluk, K. Yeliz, Ö. Orhan, Production of bone broth powder with spray drying using three different carrier agents, Korean J. Food Sci. Anim. Resour., 38 (2018) 1273–1285.
[25] R.H. Hesas, W.M.A.W. Daud, J.N. Sahu, A. Arami-Niya, The effects of a microwave heating method on the production of activated carbon from agricultural waste: a review, J. Anal. Appl. Pyrolysis,100 (2013) 1–11.
[26] B. Alhussary, A.T. Ghada, T. Amer, Preparation and characterization of natural nano hydroxyapatite from eggshell and seashell and its effect on bone healing, J. Appl. Vet. Sci., 5 (2020) 25–32.
[27] Z. Lou, H. Huang, M. Li, T. Shang, C. Chen, Controlled synthesis of carbon nanoparticles in a supercritical carbon disulfide system, J. Mater., 7 (2013) 97–105.
[28] C. Djilani, R. Zaghdoudi, F. Djazi, B. Bouchekima, A. Lallam, P.Magri, Preparation and characterisation of activated carbon from animal bones and its application for removal of organic micropollutants from aqueous solution, Desal. Water Treat., 57 (2016) 25070–25079.
[29] F. Al-Tohami, M.A. Ackacha, R.A. Belaid, M. Hamaadi, Adsorption of Zn(II) ions from aqueous solutions by novel adsorbent: ngella sativa seeds, APCBEE Procedia, 5 (2013) 400–404.
[30] G.M. Al-Senani, F.F. Al-Fawzan, Adsorption study of heavy metal ions from aqueous solution by nanoparticle of wild herbs, Egypt. J. Aquat. Res., 44 (2018) 187–194.
[31] M.A. El-Khateeb, M.A. Hussein, N.A. Sobhy, Recycling of waste chicken bones for greywater pollutants removal, Desal. Water Treat., 265 (2022) 124–133.
[32] K.H. Chu, Fitting the Gompertz equation to asymmetric breakthrough curves, J. Environ. Chem. Eng., 8 (2020) 103713, doi: 10.1016/j.jece.2020.103713.
[33] S.M. Anisuzzaman, C.G. Joseph, D. Krishnaiah, A. Bono, E. Suali, S. Abang, L.M. Fai, Removal of chlorinated phenol from aqueous media by guava seed (*Psidium guajava*) tailored activated carbon, Water Resour. Ind., 16 (2016) 29–36.
[34] M.E. Fawzy, N.M. Badr, S.I. Abou-Elela, Remediation and reuse of retting flax wastewater using activated sludge process followed by adsorption on activated carbon, Environ. Sci. Technol., 11 (2018) 167–74.
[35] M. Leili, J. Faradmal, F. Kosravian, M. Heydari, A comparison study on the removal of phenol from aqueous solution using organomodified bentonite and commercial activated carbon, Avicenna J. Environ. Health Eng., 2 (2015) 2698, doi: 10.17795/ajehe-2698.
[36] M.F. Abid, O.N. Abdulla, A.F. Kadhim, Study on removal of phenol from synthetic wastewater using solar photo catalytic reactor, J. King Saud Univ. Eng. Sci., 31 (2019) 131–139.
[37] A. Gładysz-Płaska, Application of modified clay for removal of phenol and PO_4^{3-} ions from aqueous solutions, Adsorpt. Sci. Technol., 35 (2017) 692–699.
[38] M. Malakootian, H. Jafari Mansoorian, M. Alizadeh, A. Baghbanian, Phenol removal from aqueous solution by adsorption process: study of the nanoparticles performance prepared from *Aloe vera* and *Mesquite* (*Prosopis*) leaves, Sci. Iran., 24 (2017) 3041–3052.